Head and Neck Pathol (2016) 10:1–12
DOI 10.1007/s12105-016-0686-9

SPECIAL ISSUE: SINONASAL TRACT PATHOLOGY. GUEST EDITORS: JUSTIN BISHOP, MD AND ALESSANDRO FRANCHI, MD

# Radiologic Features of Sinonasal Tumors

**Kelly K. Koeller**[1,2]

Received: 12 July 2015 / Accepted: 1 October 2015 / Published online: 1 February 2016
© Springer Science+Business Media New York 2016

**Abstract** Imaging evaluation of sinonasal tumors is most often conducted with computed tomography, which excels at identifying the effects of these masses on adjacent osseous structures, and magnetic resonance imaging that is ideal for distinguishing pathologic masses from mucosal thickening and fluid that are common in the sinonasal spaces and depicting extension into the surrounding soft tissues, orbits, and intracranial compartment. Accordingly, the two studies are complementary exams and both are commonly utilized in the assessment of these masses. Less commonly, positron emission tomography can provide additional metabolic evaluation of potential metastatic disease in patients with malignant disease. While these imaging modalities are excellent for the portrayal of an abnormality, there is considerable overlap in the imaging appearance of these tumors and specific imaging manifestations linked to a particular tumor are frequently lacking. Therefore, while the mass may be readily identified, narrowing the differential diagnosis to a single specific entity is rare. Nevertheless, cross-sectional imaging plays an essential role in patient management and valuable guidance for successful biopsy or surgical resection in virtually all cases. This review emphasizes essential imaging manifestations that correlate with sinonasal tumors in general and highlight certain features that may implicate a specific disease process.

✉ Kelly K. Koeller
koeller.kelly@mayo.edu

[1] Department of Radiology, Neuroradiology Section, American Institute for Radiologic Pathology, Silver Spring, MD, USA

[2] Mayo Clinic, 200 First Street SW, Rochester, MN, USA

**Keywords** Computed tomography · Magnetic resonance imaging · Sinonasal tumors

## Introduction

Sinonasal neoplasms are rare, accounting for 3 % of head and neck malignancies and 3.6 % of upper aerodigestive tract malignancies in the National Institutes of Health Surveillance, Epidemiology, and End Results (SEER) study [1–3]. Virtually all patients with such tumors will be evaluated with some type of radiologic examination during the course of the disease. Computed tomography (CT) and magnetic resonance imaging (MRI) are complementary modalities that excel at demonstrating the location and overall size of such masses and their potential extension into adjacent regions that may impact on surgical or therapeutic planning, particularly when they involve the anterior and middle cranial fossae, pterygopalatine fossa, orbits, or palate [1, 4, 5]. CT is often the first exam performed because of its lower cost and higher availability compared to MRI and is superior to MRI for the visualization of osseous structures. Bone erosion or remodeling is more typical for benign or slowly growing masses from pressure effects while true osseous lytic destruction is seen in higher-grade malignancies, such as squamous cell carcinoma [1]. MRI is superior to CT for identification of the soft tissue portion of most sinonasal malignancies, largely related to their T2 hypointensity that reflects hypercellularity seen on histopathology and the relative lack of fluid within these tumors. This is in juxtaposition to predominant T2 hyperintensity related to associated fluid and/or surrounding inflammatory changes or tumors of low-grade biologic activity [6]. On CT, these features are less conspicuous, causing less accurate detection of malignant

neoplasms. Furthermore, MRI may detect subtle signal changes in fatty osseous marrow (T1 hyperintense) that may herald tumor invasion either by direct geographic spread or perineural extension and which may be completely normal in appearance on CT. Perineural tumor spread is always a possibility for aggressive neoplasms arising in the nasal cavity and paranasal sinuses. Typical sites of involvement include the pterygopalatine fossa, pterygomaxillary fissure, foramen rotundum, vidian canal, inferior orbital fissure, and orbital apex [7]. All of these sites serve as regions of interest in the setting of sinonasal malignancies and the presence of such perineural involvement precludes surgical resectability. Unfortunately, small tumors may escape detection on either MRI or CT, leading to a missed opportunity for potential cure [1].

The presence of bone sclerosis on CT is typical for chronic inflammatory changes, effects of radiation therapy, and osteomyelitis but rarely noted in the setting of squamous cell carcinoma and other tumors [1]. Fibrous dysplasia, ossifying fibroma, Paget disease (sclerotic phase), and osteoblastic metastasis (usually prostate carcinoma or breast carcinoma) are other possible causes of bony sclerosis [1]. Calcifications, either from true "tumoral" calcification or residual bone, may occur in a wide variety of sinonasal tumors, including chondroid tumors (particularly along the nasal septum), fibro-osseous tumors, olfactory neuroblastoma, and inverted papilloma [1]. Despite these imaging features, very few are pathognomonic and virtually all sinonasal tumors require histopathology for specific diagnosis [1]. Positron emission tomography (PET)/CT may facilitate detection of early regional metastasis as well as more distant metastatic spread in the setting of aggressive malignancies [1].

## Selected Neoplasms

### Papilloma

Of the three distinct forms of Schneiderian papillomas, the inverted papilloma has the most highly characteristic imaging manifestation as a lobulated soft tissue mass along the lateral nasal wall and middle meatus region with a "cerebriform" appearance on T2-weighted and/or contrast-enhanced T1-weighted MR images (Fig. 1) [8, 9]. Occasional calcifications within this tumor are related to residual bone fragments [10]. Other papillomas vary in appearance, from small nasal cavity polypoid masses to those that expand the nasal cavity through pressure erosion effects and extend into the adjacent paranasal sinuses [11]. The presence of bone destruction or necrotic-appearing regions suggest more biologically aggressive disease and raise the possibility of a carcinoma [1].

### Squamous Cell Carcinoma and Adenocarcinoma

A sinonasal soft tissue mass with prominent bone destruction is a signature CT feature of squamous cell carcinoma [1, 12]. Intermediate T1 signal intensity and hypointense T2 signal (compared to fluid) with variable enhancement on contrast-enhanced T1 images that tends to be less than that of sinus mucosa are typical MRI findings (Fig. 2). Although smaller lesions are typically homogeneous in signal intensity, larger tumors are usually more heterogeneous with areas of necrosis and hemorrhage. Most squamous cell carcinomas have a nonspecific imaging appearance, making the diagnosis difficult based on the imaging findings alone [1, 13]. Skull base erosion is common with invasion into the anterior and middle cranial fossae and dural extension, best appreciated on contrast-enhanced fat-suppressed T1-weighted MRI sequences [1]. Imaging manifestations of adenocarcinoma are indistinguishable from those of squamous cell carcinoma [1].

### Salivary Tumors

A soft tissue mass arising in the palate with extension into the nasal cavity and paranasal sinuses suggests a salivary gland tumor [1]. Internally, salivary gland tumors may be heterogeneous on CT related to a variety of compositions with the more highly cellular portions being more homogeneous. Otherwise, there is considerable overlap in imaging features with other epithelial tumors in this region.

Adenoid cystic carcinoma is known for its propensity for perineural spread, which can seen as expansion of neural foramina involving the paranasal region and skull base on CT and altered signal intensity and enhancement on MRI (Fig. 3) [1]. MRI reveals intermediate T1 signal with variable T2 signal depending on the amount of cellularity (more cellular being hypointense and more stromal/less cellular being hyperintense) [14].

Most sinonasal mucoepidermoid carcinomas involve the nasal cavity and maxillary antrum [13] [1]. Pleomorphic adenoma most commonly arises from the nasal septum (90 %) and classically has a spherical morphology instead of a polypoid contour seen in many of the other epithelial tumors described previously [1].

### Neuroectodermal/Neuronal/Nerve Sheath Tumors

#### *Olfactory Neuroblastoma (Esthesioneuroblastoma)*

Correlating with clinical findings, olfactory neuroblastoma (esthesioneuroblastoma) commonly involves the superior

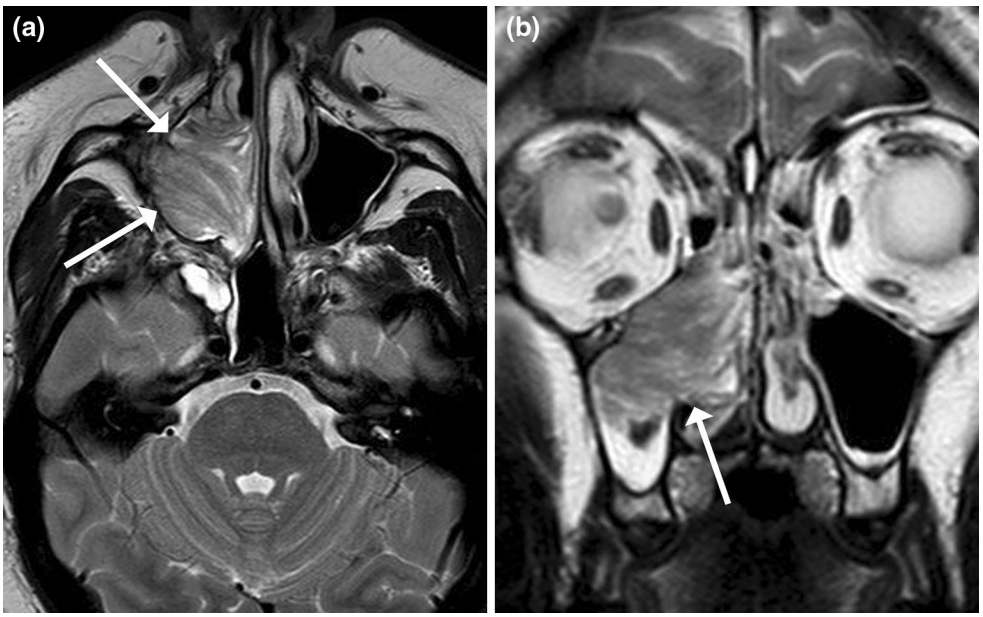


**Fig. 1** Inverted papilloma. Axial (**a**) and coronal (**b**) T2-weighted MRI images show mildly hypointense mass (*arrows*) within nasal cavity and maxillary antrum with striated "cerebriform" appearance. Case courtesy of John Lane, M.D.

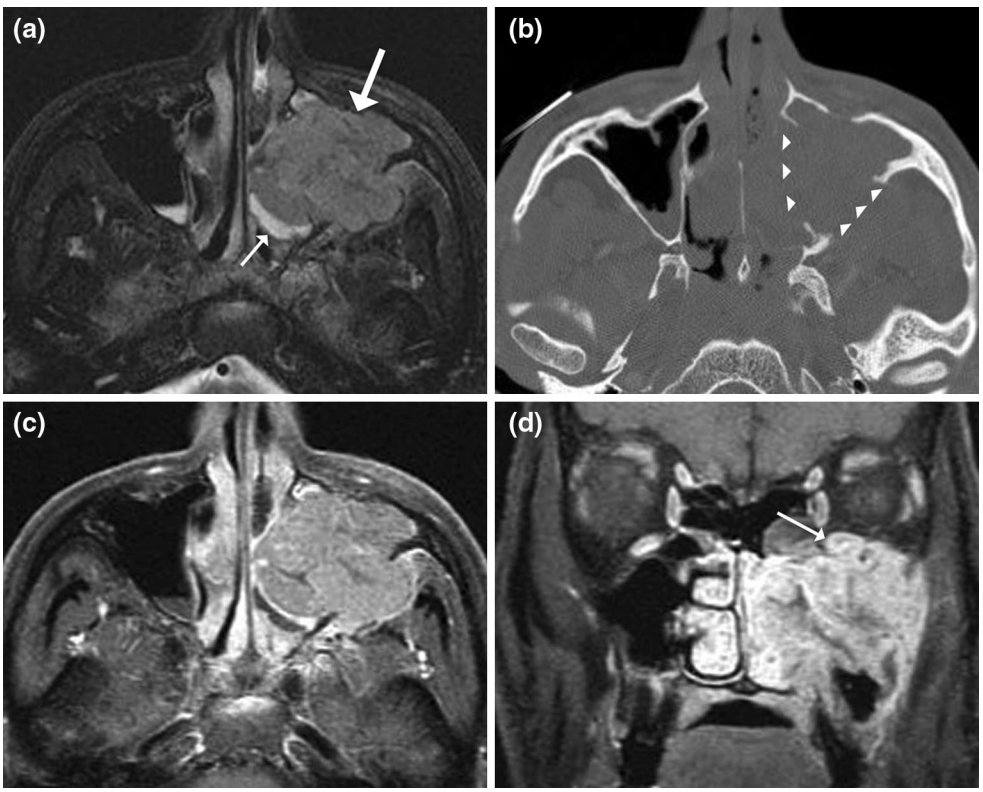


**Fig. 2** Squamous cell carcinoma. **a** Axial T2-weighted MRI image shows mildly heterogeneous hypointense mass (*arrow*) within left maxillary sinus compared to higher signal intensity of mucosal thickening/fluid (*small arrow*). **b** Axial CT image with bone windows better demonstrates associated destruction of the medial and lateral maxillary sinus walls (*arrowheads*). **c** Axial post-contrast fat-suppressed MRI image reveals intense enhancement of the mass. **d** Coronal post-contrast fat-suppressed MRI image highlights invasion into the lower left orbit with enlargement and displacement of the inferior rectus muscle (*arrow*)

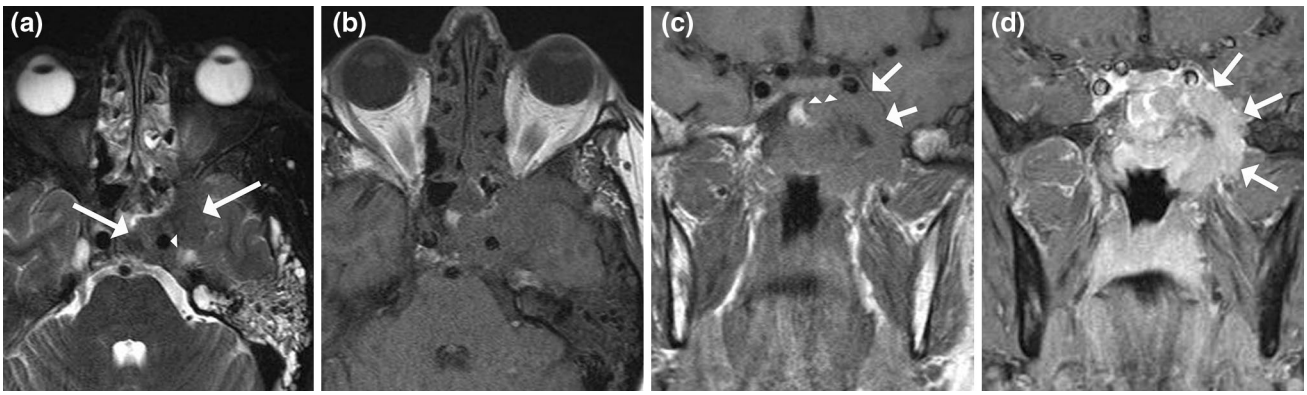


**Fig. 3** Adenoid cystic carcinoma in an adult patient with left-sided vision problems and orbital pain. **a** Axial T2-weighted MRI image show large hypointense mass (*arrows*) involving the left sphenoid sinus, cavernous sinus, adjacent middle cranial fossa and surrounding the left internal carotid artery flow void (*arrowhead*). **b** Axial T1-weighted MRI image without contrast demonstrates more homogeneous near-isointense appearance compared to muscle signal intensity. Coronal T1-weighted without contrast (**c**) and T1-weighted contrast-enhanced (**d**) MRI images better depict perineural extension along the left V3 division of the trigeminal nerve through the left foramen ovale and involvement of the cavernous sinus and left Meckel cave (*arrows*) with loss of normal signal along the sella to the left of midline (*arrowheads*)

portion of the nasal cavity and ipsilateral ethmoid and maxillary sinuses as a homogeneous enhancing expansile soft tissue mass on CT [1]. Rarely, quite prominent hyperostosis may be noted in adjacent osseous structures [15]. Heterogeneous hypointensity compared to gray matter on T1-weighted and predominant hyperintensity to gray matter on T2-weighted MRI sequences with often intense, usually homogeneous enhancement is typical. The tumor commonly invades the orbits and extends intracranially [16]. The presence of peritumoral cysts along the intracranial portion strongly suggests the diagnosis (Fig. 4) [17]. Although pathologically more similar to the olfactory neuroblastoma, sinonasal neuroendocrine carcinoma and sinonasal undifferentiated carcinoma have typical imaging appearances that are virtually indistinguishable from squamous cell carcinoma [1].

## Melanoma

The nasal cavity is the most common site in the sinonasal region for this tumor, which may less commonly involve the paranasal sinuses (maxillary more common than ethmoid) [18]. More common for those in the nasal cavity, it tends to remodel bone from pressure effects and may demonstrate a bland margin, contradicting its aggressive biologic behavior [1]. Although it may manifest with nonspecific soft tissue attenuation on CT and signal intensity on MRI, some tumors will have sufficient melanin content or hemorrhage to cause T1 hyperintensity, providing a signature (but not ubiquitous) imaging feature (Fig. 5) [1, 13]. The tumor shows usually intense but heterogeneous enhancement on post-contrast studies. Intense FDG avidity is seen on PET/CT [1]. In distinction to the nasal cavity preponderance seen in melanoma, the extremely rare melanotic neuroectodermal tumor of infancy usually arises in the maxillary sinus [1].

## Ewing Sarcoma and Primitive Neuroectodermal Tumor (PNET)

These highly malignant "small, blue, round cell tumors" are uncommon in the sinonasal region and tend to occur in children and young adults, especially in the setting of prior radiation therapy for retinoblastoma [1, 19, 20]. An aggressive imaging appearance with an expansile mass, bone destruction, and periosteal reaction ("onion-skin" more common than "sunburst") is characteristic [1].

## Peripheral Nerve Sheath Tumors

Both schwannomas and neurofibromas are common in the head and neck although only 4 % arise in the sinonasal region [21]. Reflecting its bland biologic behavior, the schwannoma manifests as a frequently ovoid well-circumscribed soft tissue mass although cystic degeneration is common with larger lesions. Subtle hyperattenuation on CT appears to correlate with regions of more densely cellular Antoni A tissue type compared to the less cellular Antoni B type. On MRI, the tumors are characterized by T1 hypointensity, T2 hyperintensity, and fairly robust enhancement on post-contrast images (Fig. 6). When cystic changes occur, areas of fluid signal intensity and surrounding peripheral ring-like enhancement are noted. Bone remodeling is the rule for these benign lesions [1, 13].

Neurofibromas are typically more heterogeneous on imaging studies compared to schwannomas with more

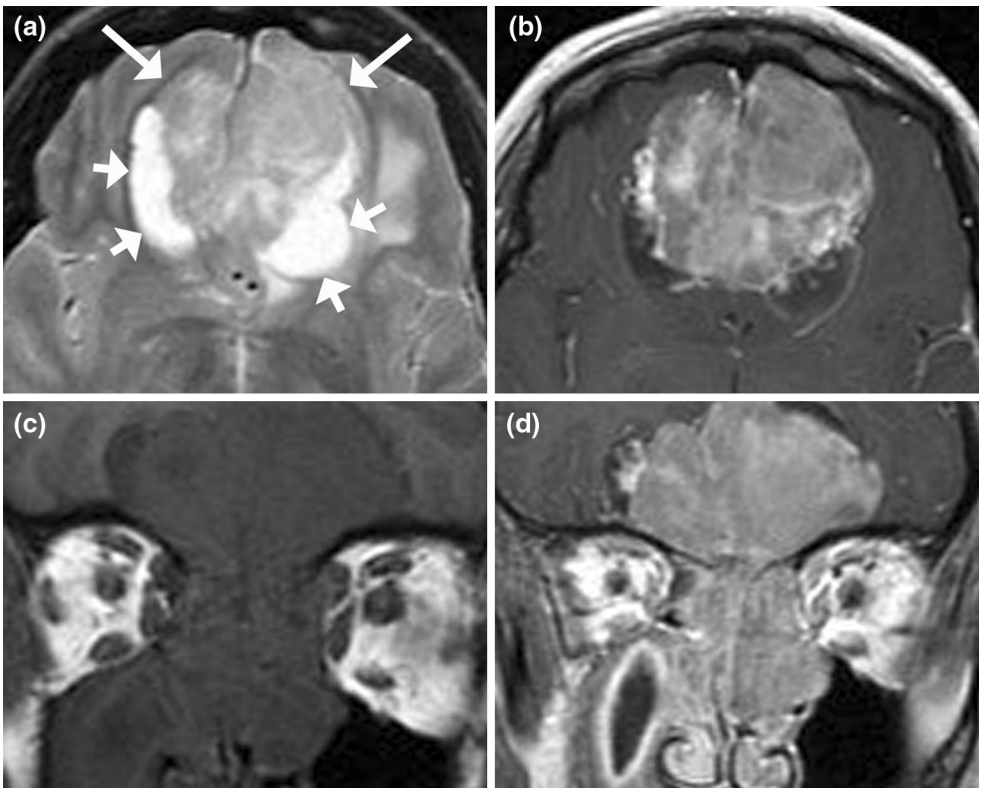


**Fig. 4** Olfactory neuroblastoma. **a** Axial T2-weighted MRI image show an inferior bifrontal heterogeneous hyperintense mass (*arrows*) with prominent surrounding hyperintense regions (*short arrows*) similar to fluid signal intensity. Coronal T1-weighted MRI image without contrast (**b**) and corresponding post-contrast fat-suppressed MRI image (**c**) demonstrates full extent of mass including involvement of the ethmoid sinuses and nasal cavity and some deformity of the medial orbital walls with intense enhancement. **d** Axial post-contrast fat-suppressed MRI image reveals intense enhancement of the mass and hypointensity of the peripheral regions. The combination of T1 hypointensity and T2 hyperintensity strongly suggests fluid, likely from cystic changes or necrosis, and the peripheral location of these collections is a characteristic imaging feature of an esthesioneuroblastoma. Case courtesy of Carrie Carr, M.D.

intermediate T1 signal and heterogeneous enhancement. Some plexiform neurofibromas may have an imaging appearance suggesting a "bag of worms" morphology [1].

As its name implies, malignant peripheral nerve sheath tumor is a much more aggressive tumor than the benign varieties of nerve sheath tumors described above and tends to show imaging manifestations that are more similar to those of squamous cell carcinoma [1].

## Tumors of the Central Nervous System

A variety of neoplasms from the central nervous system may involve the sinonasal region by direct extension or arising from embryologic remnants. These include but are not limited to meningioma, craniopharyngioma, chordoma, and nasal glioma. Most sinonasal meningiomas arise from intracranial tumors with direct extension across the skull base. An intensely enhancing dural-based mass with signal intensity similar to that of brain on MRI is typically seen. Much more rarely, an isolated meningioma in the sinonasal region may be encountered, presumably arising from arachnoid cap cells trapped in this region during embryogenesis [1]. Altered contour, CT hypoattenuation, scattered calcifications, and quite variable altered signal intensity on MRI of the clivus should raise concern for a chordoma, although chondrosarcoma and metastatic disease are also diagnostic considerations. If a chordoma is large enough to involve the paranasal sinuses, the entire clivus, including its tip, should be involved as well [1]. Rarely, isolated chordomas within the paranasal sinuses have been reported and presumably arise from ectopic embryologic rests as a result of descent of the notochord into the developing facial region in utero [1, 22, 23]. A cribriform plate defect with a soft tissue sinonasal mass is a classic imaging manifestation of a nasal glioma [1].

## Lymphoma

In general, B cell lymphoma tends to involve the paranasal sinuses and predominate in Western populations while T-cell lymphoma (especially nasal T/NK-cell lymphoma) is the most common to involve the nasal cavity with a predilection for Asian and South American populations [1, 24, 25]. Both types are known for producing bulky soft

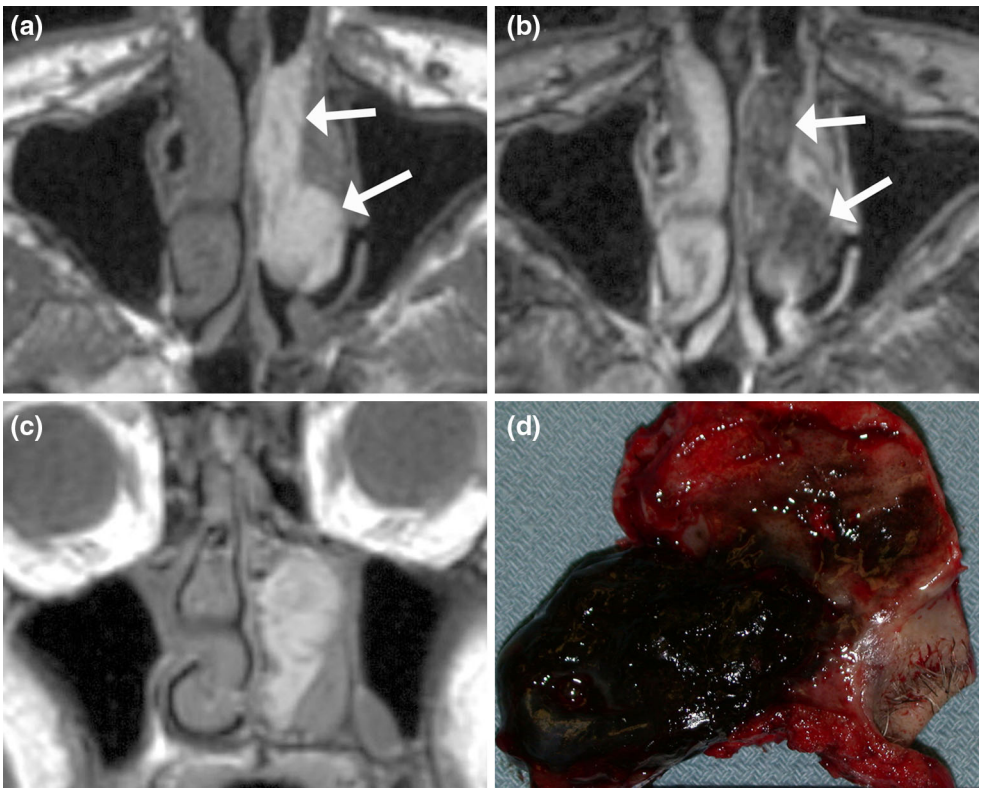


**Fig. 5** Melanoma arising in the nasal cavity. **a** Axial T1-weighted MRI image shows mildly heterogeneous hyperintense mass (*arrows*) within left nasal cavity compared to lower signal intensity of nasal turbinates. **b** Axial T2-weighted MRI image demonstrates corresponding hypointensity of the mass (*arrows*). **c** Coronal T1-weighted MRI image without contrast depicts involvement of both left middle and inferior turbinates. **d** Surgical specimen photograph shows markedly darkened pigmentation that corresponded with the region of T1 hyperintensity. The combination of the imaging and gross pathology findings is highly characteristic for melanoma

tissue masses that tend to remodel bone although lytic destruction can be seen, particularly with the nasal T/NK-cell variety [1, 24, 26]. The nasal cavity and maxillary sinus are the most common locations of the disease [24]. The masses tend to be isointense to muscle on T1-weighted and mildly hyperintense to muscle and hypointense to mucosa on T2-weighted imaging with at least moderate enhancement on post-contrast T1-weighted imaging (Fig. 7) [24, 26].

Other diseases involving the nasal cavity and paranasal sinuses with similar imaging manifestations as lymphoma include Wegener granulomatosis, multiple myeloma/extramedullary plasmacytoma, and chloroma [1, 27]. In the sinonasal region, Rosai-Dorfman disease frequently mimics the imaging appearance of lymphoma with the frequent addition of prominent cervical adenopathy and multifocal extranodal lesions [28–30].

## Langerhans Cell Histiocytosis

This group of childhood diseases commonly involves the head and neck, particularly the flat bones of the skull and jaw, but is rarely seen in the sinonasal region. A well-defined soft tissue mass with local osseous destruction is typical [31, 32]. Isointense signal on T1-weighted and isointense-to-hyperintense signal on T2-weighted imaging compared to white matter with intense enhancement has been reported [32].

## Juvenile Nasopharyngeal Angiofibroma and Other Vascular Tumors

Juvenile nasopharyngeal angiofibroma is a highly vascular soft tissue mass with a highly characteristic imaging appearance because of its consistent nasopharyngeal location near the sphenopalatine foramen causing expansion of the pterygopalatine fossa and anterior bowing of the ipsilateral posterior maxillary sinus wall (Fig. 8). The combination of these features in an adolescent male strongly suggests the diagnosis [33]. Extension through the roof of the sphenoid sinus frequently occurs with less common involvement of the maxillary and ethmoid sinuses [34]. The tumor may also extend into the orbit and then into the intracranial compartment via the superior and inferior orbital fissures [1, 13]. MRI shows intermediate T1 and T2 signal intensity with multiple flow-voids, usually from

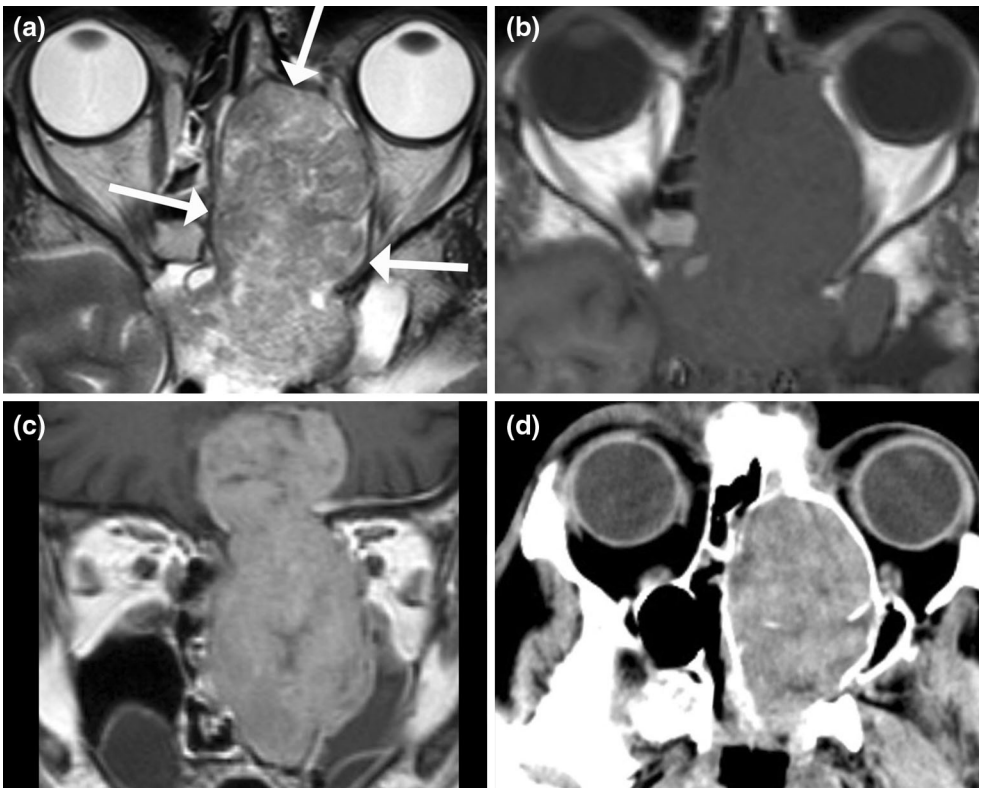


**Fig. 6** Schwannoma. **a** Axial T2-weighted MRI image show heterogeneous hyperintense mass (*arrows*) within left ethmoid and sphenoid sinuses and nasal cavity. **b** Axial T1-weighted MRI image without contrast demonstrates more homogeneous hypointensity compared to extraocular muscle signal intensity. **c** Coronal post-contrast MRI image highlights invasion across the skull base into the anterior cranial fossa. **d** Axial CT image with soft tissue windows better demonstrates associated expansion of the osseous structures related to pressure erosion effects (rather than bony destruction), strongly favoring a benign process and typical for a nerve sheath tumor

internal maxillary artery feeding vessels [13]. CT frequently demonstrates deossification of the adjacent skull base [1].

Although occasionally confused for an angiofibroma, the angiomatous polyp is a distinct entity believed to result from a fibrosed, vascularized nasal polyp following minor trauma. This tumor is much less vascular than the angiofibroma, is found in the nasal cavity instead of the nasopharynx, does not extend into the pterygopalatine fossa, and rarely extends into the sphenoid sinus [33].

Most nasal cavity hemangiomas involve the septum and inferior and middle turbinates with the lateral wall and vestibule less common locations [1]. They are often difficult to identify as discrete lesions from the turbinates, as both enhance intensely on post-contrast imaging. Occasional flow voids may be noted on MRI [1]. When they arise intraosseously, a "sunburst", "soap bubble", "radiating", or "honeycomb" appearance is characteristic on CT using bone windows with T1 hypointensity, T2 hyperintensity, and intense enhancement on post-contrast imaging (Fig. 9) [35].

Hemangiopericytoma tends to occur in the nasal fossa and maxillary sinus as an enhancing soft tissue mass causing bone remodeling without specific CT or MRI features. Flow voids may be present [36].

## Muscle and Fibroblastic Tumors

Head and neck rhabdomyosarcoma is most commonly seen in the orbit and nasopharynx but 12 % of those arising in children involve the sinonasal cavities [37]. Although the tumor is overall more common in children, a wider age range is seen for those arising in the sinonasal region [38, 39]. Bone remodeling and bone destruction frequently occur together. CT and MRI imaging characteristics are otherwise not specific with homogeneous signal intensity on MRI and enhancement on post-contrast imaging (Fig. 10). On occasion, it may mimic the appearance of a squamous cell carcinoma [1].

While grade II/III fibrosarcomas are more common as mandibular tumors, the grade I fibrosarcoma (desmoid tumor) is more common in the sinonasal region and more commonly seen in children. The tumor is usually homogeneous on CT with low-to-intermediate signal on T1 and T2 MRI sequences and minimal enhancement [1].

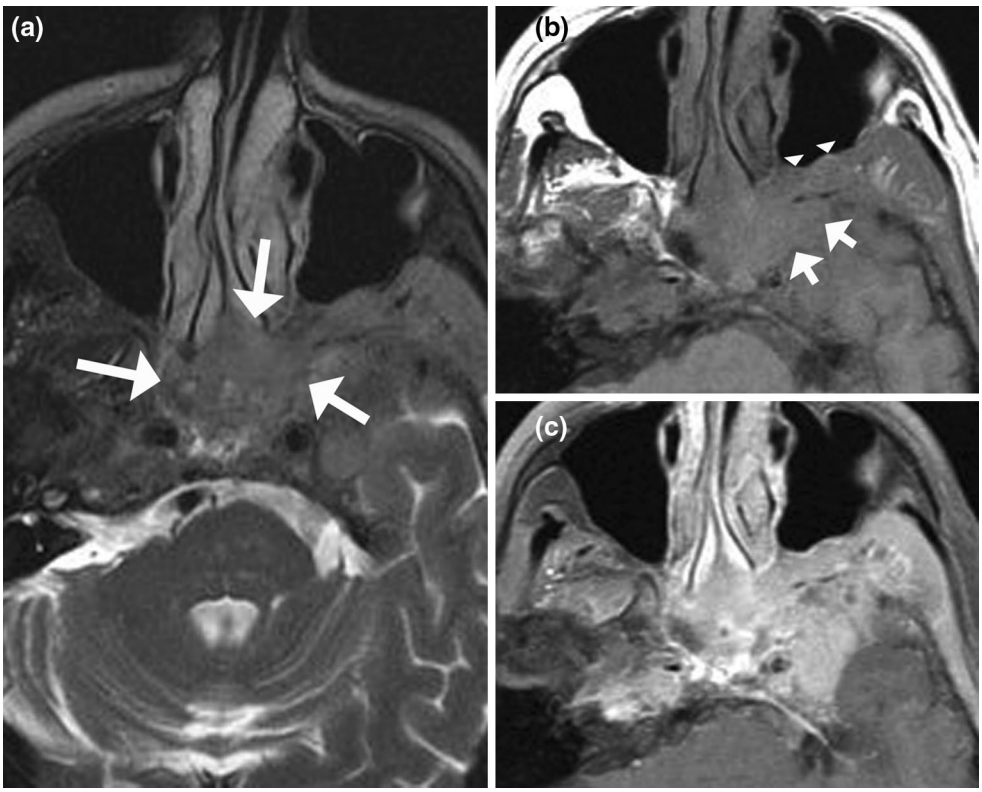


**Fig. 7** Lymphoma. **a** Axial T2-weighted MRI image shows a soft tissue mass slightly hyperintense compared to muscle (*arrows*) involving the left ethmoid sinus and cavernous sinus. **b** Axial T1-weighted MRI image without contrast better demonstrates involvement of the left pterygopalatine fossa (*arrowheads*), and middle cranial fossa (*short arrows*). **c** Post-contrast fat-suppressed axial T1-weighted MRI image reveals intense enhancement of the mass

Fibromyxomas and myxomas are locally aggressive soft tissue masses when they arise in the sinonasal region. Focal bone destruction and flecks or strands of calcification in an otherwise cyst-like mass on CT are common. Mildly heterogeneous T1 hypointensity and T2 hyperintensity with intense enhancement is seen on MRI. The CT appearance may mimic that of a fibrosarcoma [1].

## Osseous Lesions and Tumors

Osseous and fibroosseous lesions comprise nearly 25 % of nonepithelial tumors involving the sinonasal cavities [1].

Osteomas are most common within the frontal sinuses followed by the ethmoid sinuses and rarely involve the maxillary or sphenoid sinuses [40]. This benign intraosseous proliferation of mature bone arises from the sinus wall, is nearly always limited to the sinus contour but can be a source of spontaneous cerebrospinal fluid rhinorrhea and pneumocephalus, often related to a defect of the ethmoid complex or sphenoid sinus [1]. While their detection is straightforward on CT with hyperattenuation, they may be completely inconspicuous on non-contrast MRI related to heterogeneous low-to-intermediate signal intensity but with at least some enhancement on post-contrast MRI [1, 13]. Multiple osteomas may reflect Gardner syndrome, a familial polyposis associated with intestinal polyps and benign skin and subcutaneous neoplasms [1, 41].

Osteochondromas, believed to represent a developmental variation and arise from the bony surface with a cartilage cap, are rare in the sinonasal region. Known for their pedunculated mushroom shape, they commonly show heterogeneous low-to-intermediate signal intensity on MRI [1].

Chondroma is expansile circumscribed tumors of cartilaginous origin that may remodel bone as they grow. Reflecting a benign biologic behavior, it should not demonstrate any bone destruction on CT. The tumor rarely involves the sinonasal region. Calcifications are common but may not always be detected on CT. Nonspecific T1 hypointensity, T2 hyperintensity, and enhancement on post-contrast images are seen on MRI [1]. An osteoma may have a similar appearance with the exception of more coarsely organized calcifications and a dense bony "cap" [1, 42]. More worrisome, a chondrosarcoma may mimic the imaging appearance of a chondroma [13].

Sinonasal ossifying fibroma manifests as an expansile circumscribed mass with characteristic (but not ubiquitous) internal calcifications and a thick bony shell representing

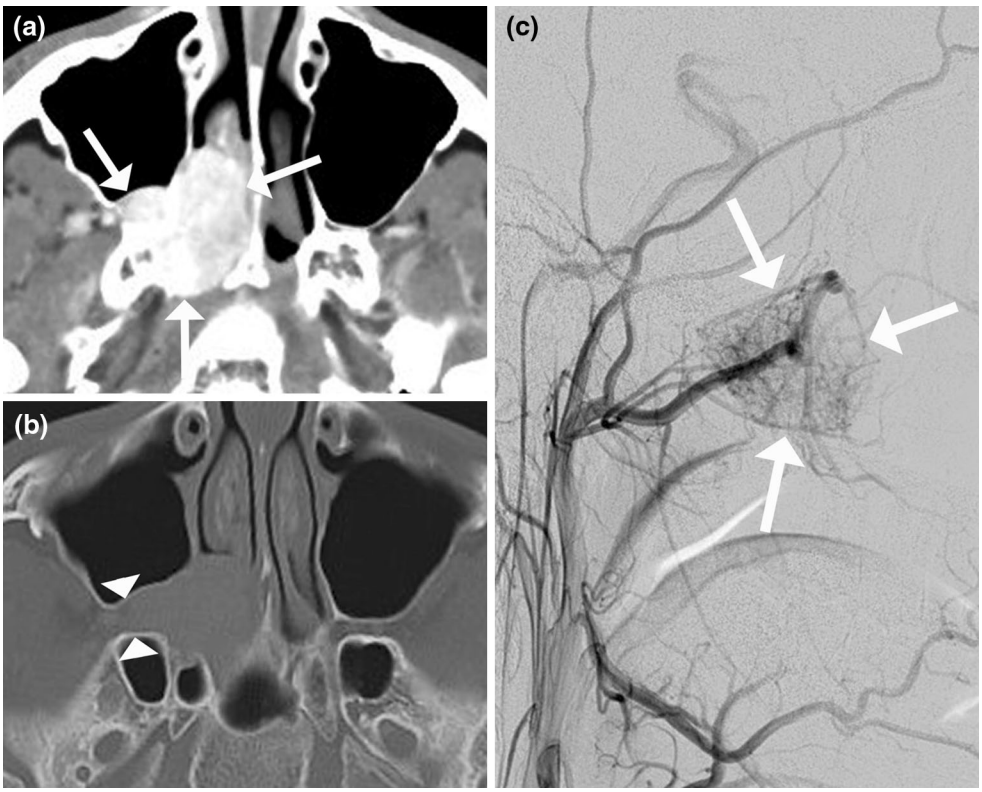


**Fig. 8** Juvenile nasopharyngeal angiofibroma. **a** Axial CT image with contrast shows enhancing soft tissue mass (*arrows*) centered in the right nasopharyngeal region with extension into the adjacent pterygopalatine fossa (*arrowheads*) and nasal choana. **b** Axial CT image with bone windows better demonstrates expansion of these regions related to pressure erosion effects, strongly implicating a benign biologic process. **c** Lateral angiographic image reveals intense blush of the mass (*arrows*) in the arterial phase. The combination of these imaging findings is highly characteristic for a juvenile nasopharyngeal angiofibroma. Case courtesy of Harry Cloft, M.D., Ph.D.

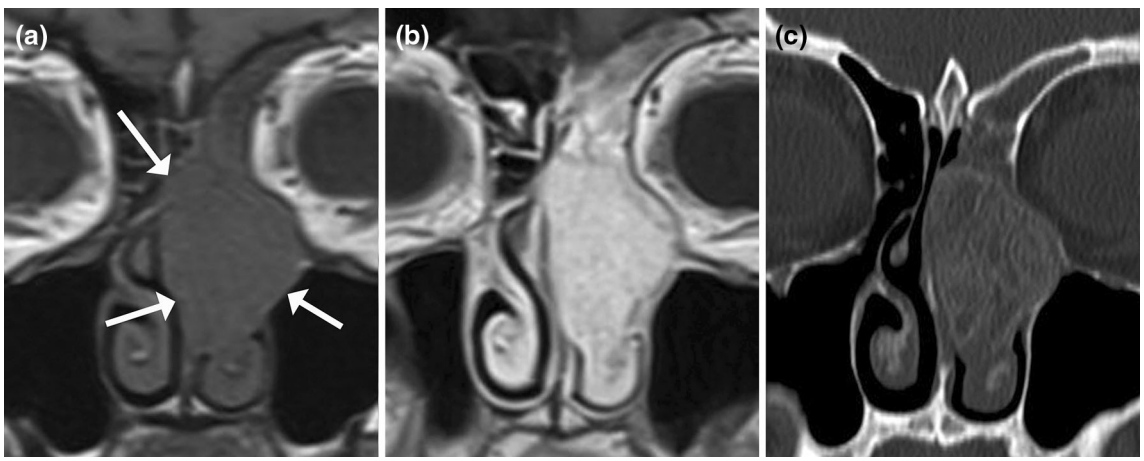


**Fig. 9** Intraosseous hemangiomas involving middle turbinate. **a** Coronal T1-weighted MRI image without contrast shows diffusely hypointense mass (*arrows*) centered in the region of the left middle turbinate. **b** Contrast-enhanced coronal T1-weighted MRI image reveals intense but nonspecific enhancement. **c** Coronal CT image with bone windows demonstrates characteristic "honeycomb" ossification pattern within the mass, favoring the diagnosis of an intraosseous hemangioma. Case courtesy of Steven Weindling, M.D.

reactive bony change rather than actual tumor [43–45]. A sharp transition at the bony margin distinguishes this lesion from the more ill-defined transition seen in fibrous dysplasia [43]. Nonossified areas corresponding to hemorrhagic or proteinaceous content may be occasionally seen on CT and likely also contribute to a variable MRI

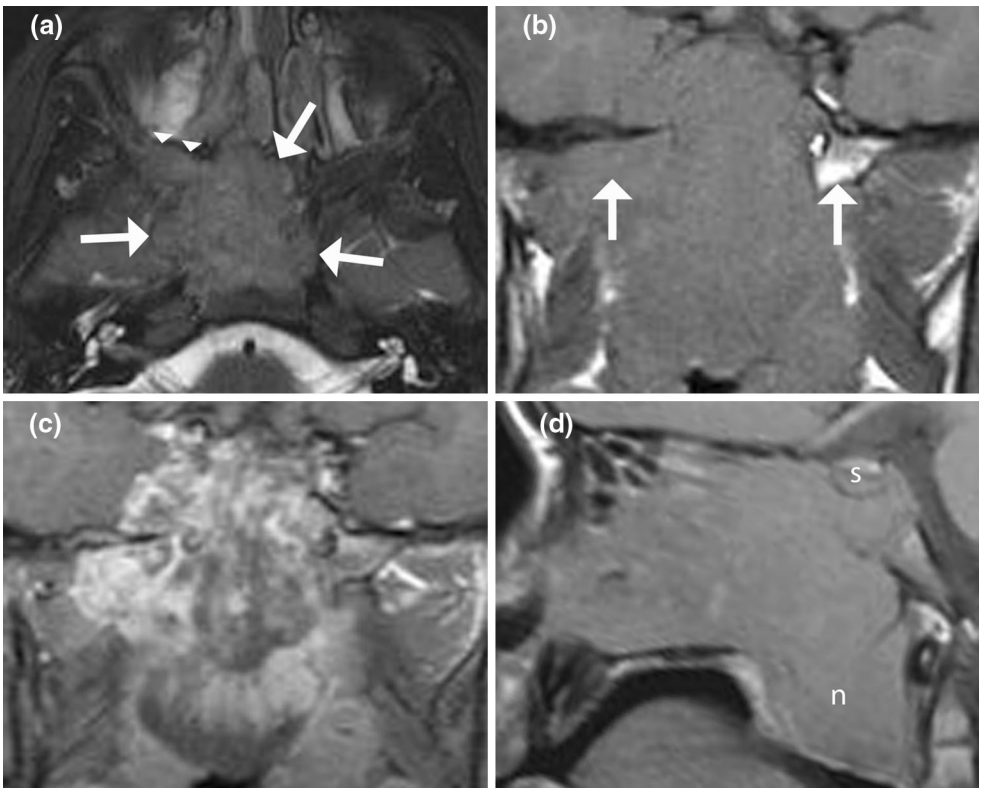


**Fig. 10** Rhabdomyosarcoma in a 4-year-old with sinus congestion. **a** Axial T2-weighted MRI image shows large mildly hyperintense mass (*arrows*) involving the central skull base, nasopharynx, and posterior nasal cavity with extension into the right pterygopalatine fossa (*arrowheads*). **b** Coronal T1-weghted MRI image without contrast demonstrates corresponding hypointensity and better depiction of destruction of the right sphenoid wing (compare to normal fat signal of left sphenoid wing, *small arrows*) and extension into the right middle cranial fossa. **c** Contrast-enhanced fat-suppressed coronal T1-weighted MRI image reveals intense but heterogeneous enhancement of the mass. **d** Sagittal T1-weighted MRI image highlights inferior extension into nasopharynx (n) and replacement of the sphenoid bone along the sella (s) margin

appearance with isointense-to-hyperintense T1 signal intensity, usually hypointense T2 signal intensity, and moderate contrast-enhancement that is particularly prominent along the periphery of the mass [43, 44]. A variant form, psammomatoid active ossifying fibroma, shares many imaging features of the ossifying fibroma but typically shows a more aggressive imaging appearance with prominent osseous expansion and cortical disruption [41].

Fibrous dysplasia commonly involves craniofacial bones and impacts on the sinonasal region. As a result of poorly organized fibroosseous tissue replacing normal medullary bone, a variety of CT imaging manifestations—ranging from marked heterogeneity from a mixture of osseous and fibrous matrix to the classic "ground glass" appearance—are possible and reflect the stage of development and amount of bony matrix within the lesion [13]. On MRI, predominant T1 and T2 hypointense signal with intense enhancement on post-contrast imaging is typical. Associated mucoceles are occasionally noted [46, 47]. Both fibrous dysplasia and ossifying fibroma may mimic the imaging appearance of a meningioma [41].

Osteogenic sarcoma and chondrosarcoma are aggressive malignancies known for bone destruction and heterogeneity on CT and MRI with typically intense enhancement. The tumors uncommonly involve the sinonasal region. An association with suture margins (such as those involving the facial bones or nasal septum) and curvilinear calcifications are imaging findings that favor a chondrosarcoma, especially one of lower-grade [13]. "Sunburst" periosteal reaction favors an osteogenic sarcoma. Prior radiation therapy for retinoblastoma is a predisposing factor for an osteogenic sarcoma in this region [1].

## Summary

The vast majority of sinonasal neoplasms have a nonspecific imaging appearance. Effects of these masses on adjacent osseous structures may favor a benign lesion (with pressure erosion changes), a malignant lesion (with lytic destruction), or a sarcoma (with periosteal reaction). Evidence of perineural extension strongly supports the

presence of an aggressive neoplasm and is a significant imaging finding for patient management. Notable imaging manifestations that may suggest a specific diagnosis include the "cerebriform" appearance of the inverted papilloma, T1 hyperintensity in the setting of melanoma, the presence of a calcified rim in the ossifying fibroma, and characteristic locations such as the superior portion of the nasal cavity for the esthesioneuroblastoma and nasopharynx/pterygopalatine fossa for the juvenile nasopharyngeal angiofibroma.

**Acknowledgments** The author acknowledges contributions of case material to the Armed Forces Institute of Pathology and American Institute for Radiologic Pathology from radiology residents worldwide and from colleagues at the Mayo Clinic.

## References

1. Som PM, Brandwein-Gensler MS, Kassel EE, Genden EM. Tumors and tumor-like conditions of the sinonasal cavities. In: Som PM, Curtin HD, editors. Head and neck imaging. 5th ed. St Louis: Elsevier; 2011. p. 253–410.
2. Batsakis J. Tumors of the head and neck: clinical and pathological considerations. 2nd ed. Baltimore: Williams and Wilkins; 1979. p. 177–87.
3. Muir C, Weiland L. Upper aerodigestive tract cancers. Cancer. 1995;75(1 Suppl):147–53.
4. Nishijima W, Takooda S, Tokita N, Takayama S, Sakura M. Analyses of distant metastases in squamous cell carcinoma of the head and neck and lesions above the clavicle at autopsy. Arch Otolaryngol Head Neck Surg. 1993;119(1):65–8.
5. Jeans WD, Gilani S, Bullimore J. The effects of CT scanning on staging of tumours of the paranasal sinuses. Clin Radiol. 1982;33(2):173–9.
6. Som PM, Shapiro MD, Biller HF, Sasaki C, Lawson W. Sinonasal tumors and inflammatory tissues: differentiation with MR imaging. Radiology. 1988;167(3):803–8.
7. Loevner LA, Sonners AI. Imaging of neoplasms of the paranasal sinuses. Neuroimaging Clin N Am. 2004;14(4):625–46.
8. Dammann F, Pereira P, Laniado M, Plinkert P, Lowenheim H, Claussen CD. Inverted papilloma of the nasal cavity and the paranasal sinuses: using CT for primary diagnosis and follow-up. AJR Am J Roentgenol. 1999;172(2):543–8.
9. Ojiri H, Ujita M, Tada S, Fukuda K. Potentially distinctive features of sinonasal inverted papilloma on MR imaging. AJR Am J Roentgenol. 2000;175(2):465–8.
10. Lund VJ, Lloyd GA. Radiological changes associated with inverted papilloma of the nose and paranasal sinuses. Br J Radiol. 1984;57(678):455–61.
11. Momose KJ, Weber AL, Goodman M, MacMillan AS Jr, Roberson GH. Radiological aspects of inverted papilloma. Radiology. 1980;134(1):73–9.
12. Chaudhry AP, Gorlin RJ, Mosser DG. Carcinoma of the antrum: a clinical and histopathologic study. Oral Surg Oral Med Oral Pathol. 1960;13:269–81.
13. Mafee MF. Imaging of the nasal cavity and paranasal sinuses. In: Mafee MF, Valvassori GE, Becker M, editors. Imaging of the head and neck. 2nd ed. Sttutgart: Thieme; 2005. p. 412–66.
14. Sigal R, Monnet O, de Baere T, et al. Adenoid cystic carcinoma of the head and neck: evaluation with MR imaging and clinical-pathologic correlation in 27 patients. Radiology. 1992;184(1):95–101.
15. Regenbogen VS, Zinreich SJ, Kim KS, et al. Hyperostotic esthesioneuroblastoma: CT and MR findings. J Comput Assist Tomogr. 1988;12(1):52–6.
16. Derdeyn CP, Moran CJ, Wippold FJ 2nd, Chason DP, Koby MB, Rodriguez F. MRI of esthesioneuroblastoma. J Comput Assist Tomogr. 1994;18(1):16–21.
17. Som PM, Lidov M, Brandwein M, Catalano P, Biller HF. Sinonasal esthesioneuroblastoma with intracranial extension: marginal tumor cysts as a diagnostic MR finding. AJNR Am J Neuroradiol. 1994;15(7):1259–62.
18. Freedman HM, DeSanto LW, Devine KD, Weiland LH. Malignant melanoma of the nasal cavity and paranasal sinuses. Arch Otolaryngol. 1973;97(4):322–5.
19. Klein EA, Anzil AP, Mezzacappa P, Borderon M, Ho V. Sinonasal primitive neuroectodermal tumor arising in a long-term survivor of heritable unilateral retinoblastoma. Cancer. 1992;70(2):423–31.
20. Lane S, Ironside JW. Extra-skeletal Ewing's sarcoma of the nasal fossa. J Laryngol Otol. 1990;104(7):570–3.
21. Hillstrom RP, Zarbo RJ, Jacobs JR. Nerve sheath tumors of the paranasal sinuses: electron microscopy and histopathologic diagnosis. Otolaryngol Head Neck Surg. 1990;102(3):257–63.
22. Miro JL, Videgain G, Petrenas E, et al. Chordoma of the ethmoidal sinus. A case report. Acta Otorrinolaringologica Espanola. 1998;49(1):66–9.
23. Shugar JM, Som PM, Krespi YP, Arnold LM, Som ML. Primary chordoma of the maxillary sinus. Laryngoscope. 1980;90(11 Pt 1):1825–30.
24. Ooi GC, Chim CS, Liang R, Tsang KW, Kwong YL. Nasal T-cell/natural killer cell lymphoma: CT and MR imaging features of a new clinicopathologic entity. AJR Am J Roentgenol. 2000;174(4):1141–5.
25. Cleary KR, Batsakis JG. Sinonasal lymphomas. Ann Otol Rhinol Laryngol. 1994;103(11):911–4.
26. King AD, Lei KI, Ahuja AT, Lam WW, Metreweli C. MR imaging of nasal T-cell/natural killer cell lymphoma. AJR Am J Roentgenol. 2000;174(1):209–11.
27. Borges A, Fink J, Villablanca P, Eversole R, Lufkin R. Midline destructive lesions of the sinonasal tract: simplified terminology based on histopathologic criteria. AJNR Am J Neuroradiol. 2000;21(2):331–6.
28. Gregor RT, Ninnin D. Rosai-Dorfman disease of the paranasal sinuses. J Laryngol Otol. 1994;108(2):152–5.
29. Ku PK, Tong MC, Leung CY, Pak MW, van Hasselt CA. Nasal manifestation of extranodal Rosai-Dorfman disease–diagnosis and management. J Laryngol Otol. 1999;113(3):275–80.
30. Wenig BM, Abbondanzo SL, Childers EL, Kapadia SB, Heffner DR. Extranodal sinus histiocytosis with massive lymphadenopathy (Rosai-Dorfman disease) of the head and neck. Hum Pathol. 1993;24(5):483–92.
31. Hussain SS, Simpson RD, McCormick D, Johnstone CI. Langerhan's cell histiocytosis in the sphenoid sinus: a case of diabetes insipidus. J Laryngol Otol. 1989;103(9):877–9.
32. Stromberg JS, Wang AM, Huang TE, Vicini FA, Nowak PA. Langerhans cell histiocytosis involving the sphenoid sinus and superior orbital fissure. AJNR Am J Neuroradiol. 1995;16(4 Suppl):964–7.
33. Som PM, Cohen BA, Sacher M, Choi IS, Bryan NR. The angiomatous polyp and the angiofibroma: two different lesions. Radiology. 1982;144(2):329–34.
34. Apostol JV, Frazell EL. Juvenile nasopharyngeal angiofibromaA clinical study. Cancer. 1965;18:869–78.

35. Goff R, Weindling S, Gupta V, Nassar A. Intraosseous hemangioma of the middle turbinate: a case report of a rare entity and literature review. Neuroradiol J. 2015;28:148–51.
36. Herve S, Abd AI, Beautru R, et al. Management of sinonasal hemangiopericytomas. Rhinology. 1999;37(4):153–8.
37. Anderson GJ, Tom LW, Womer RB, Handler SD, Wetmore RF, Potsic WP. Rhabdomyosarcoma of the head and neck in children. Arch Otolaryngol Head Neck Surg. 1990;116(4):428–31.
38. Callender TA, Weber RS, Janjan N, et al. Rhabdomyosarcoma of the nose and paranasal sinuses in adults and children. Otolaryngol Head Neck Surg. 1995;112(2):252–7.
39. Lee JH, Lee MS, Lee BH, et al. Rhabdomyosarcoma of the head and neck in adults: MR and CT findings. AJNR Am J Neuroradiol. 1996;17(10):1923–8.
40. Chen CY, Ying SH, Yao MS, Chiu WT, Chan WP. Sphenoid sinus osteoma at the sella turcica associated with empty sella: CT and MR imaging findings. AJNR Am J Neuroradiol. 2008;29(3):550–1.
41. Wenig BM, Mafee MF, Ghosh L. Fibro-osseous, osseous, and cartilaginous lesions of the orbit and paraorbital region Correlative clinicopathologic and radiographic features, including the diagnostic role of CT and MR imaging. Radiol Clin N Am. 1998;36(6):1241–59.
42. Osguthorpe JD, Hungerford GD. Benign osteoblastoma of the maxillary sinus. Head Neck Surg. 1983;6(1):605–9.
43. Han MH, Chang KH, Lee CH, Seo JW, Han MC, Kim CW. Sinonasal psammomatoid ossifying fibromas: CT and MR manifestations. AJNR Am J Neuroradiol. 1991;12(1):25–30.
44. Engelbrecht V, Preis S, Hassler W, Lenard HG. CT and MRI of congenital sinonasal ossifying fibroma. Neuroradiology. 1999; 41(7):526–9.
45. Wenig BM, Vinh TN, Smirniotopoulos JG, Fowler CB, Houston GD, Heffner DK. Aggressive psammomatoid ossifying fibromas of the sinonasal region: a clinicopathologic study of a distinct group of fibro-osseous lesions. Cancer. 1995;76(7):1155–65.
46. Som PM, Lidov M. The benign fibroosseous lesion: its association with paranasal sinus mucoceles and its MR appearance. J Comput Assist Tomogr. 1992;16(6):871–6.
47. Sterling KM, Stollman A, Sacher M, Som PM. Ossifying fibroma of sphenoid bone with coexistent mucocele: CT and MRI. J Comput Assist Tomogr. 1993;17(3):492–4.